4.6 Thermodynamic Evaluation during the Reduction of MWO4 (M = Fe, Mn, Zn) with Methane for the Production of Hydrogen-Syngas

V. Collins-Martínez, M. J. Meléndez-Zaragoza, A. López-Ortiz

Departamento de Ingeniería y Química de Materiales, Centro de Investigación en Materiales Avanzados, S.C., Miguel de Cervantes 120, Chihuahua, Chih., México, 31136, México.

ABSTRACT

Different types of MWO_4 (M = Fe, Mn, Ni) were evaluated through thermodynamic analysis and process simulation for the production of hydrogen-synthesis gas (syngas). The partial oxidation (POX) of methane is a more efficient reaction than steam reforming (SMR). However, currently the dominant technology in hydrogen production is through SMR. To overcome one of the most important disadvantages of POX reaction, which deals with the use of pure oxygen as a gas feed, a mixed metal oxide (MWO_4, M = Fe, Mn, Ni) is proposed as an oxygen carrier (POX-MeO). The aim of the present study is to evaluate the feasibility of these tungstate metal oxides through the use of thermodynamic analyses and process simulations of an arrangement of two reactors. In the first reactor POX-MeO reactions ($CH_4 + MWO_4 = H_2 + CO + M + W$; $CH_4 + MWO_4 = H_2 + CO_2 + M + W$) and the undesirable coal formation ($CH_4 = C + 2H_2$) are carried out. While in the second reactor, solid products of the first reactor are combined with steam to gasify the previously deposited coal ($C + H_2O = H_2 + CO$; $C + 2H_2O = 2H_2 + CO_2$) and simultaneously regenerate the metal oxide to produce syngas ($M + W + H_2O = MWO_4 + H_2$). Then, the regenerated oxide is recycled back to the first reactor to make a continuous process. Results of simulation of this process with the different MWO_4 oxides are presented using Aspen Plus.

Keywords:Thermodynamicanalysis, chemical looping, tungstate oxides, hydrogen production, syngas.

1. Introduction

Despite the current weakness of world energy markets and the sluggish Chinese growth, demand for energy will continue to grow over the next 20 years and even later as

the world economy expands and more energy is needed to push for greater industrial activity. According to the 2016 BP World Energy Outlook [1], global energy demand is expected to increase by 34% between 2014 and 2035, at an average of 1.4% per year. This growth in demand generally includes significant changes in the composition of the energy mix, with faster growth of low-carbon fuels than those with higher emissions as the planet begins the transition to a future with lower carbon emissions.

Even though the fast growth in other energy sources, it is predicted that fossil fuels will continue to be the predominant form of energy by 2035, accounting for 60% of the expected increase in demand and almost 80% of the world's total energy supply by 2035.Natural gas will be the fastest growing fossil fuel, with an annual increase of 1.8%, and oil will grow at a constant rate of 0.9% per year, although its share in the energy mix will continue to decline. Coal growth is expected to decline dramatically, so that by 2035 its share of the energy mix will be the lowest ever, being replaced by gas as the second largest source of fuel. Furthermore, natural gas supply is growing strongly thanks to a large increase in the production of shale gas worldwide, which is expected to grow by 5.6% annually. The share of shale gas in total gas production will increase from 10% in 2014 to almost 25% in 2035 [1].

Moreover, hydrogen has been employed as a common raw material for a wide variety of processes, for example, in ammonia synthesis, pharmaceuticals, hydrogen peroxide generation,electronics and petrochemical industries [2, 3]. Nowadays, hydrogen has been considered as aclean, renewable and efficient fuel since, when used in combination with fuel cells, hydrogen can produce heat and electricity with the only waste being pure water. The fact that hydrogen is not a primary energy source like most common fossil fuels (coal or natural gas) makes it an energy vector that can be produced from many traditional energy systems (most hydrogen today is produced from natural gas). However, in order for hydrogen to be considered as a clean fuel this must come from renewable energy sources.

Furthermore, of comparable importance to hydrogen, the mixture of hydrogen and carbon monoxide (H_2 + CO), commonly called synthesis gas or syngas [4-6] is a valuable raw material for various industrial applications.Technically, syngas can be generated from any hydrocarbon feedstock [7]. However, in most applications, natural gas is the predominant raw material [4].

Steam reforming of natural gas (mainly methane, SMR, reaction 1) is the main process for the production of syngas [7-10]. However, partial oxidation of methane (POX, reaction 2) for the production of syngas has been reported to present higher efficiencies than SMR [11]. Furthermore, POX exhibits other benefits such as: less investment required to produce a syngas at a molar ratio of H_2/CO = 2, an inherent exothermic reaction of this process, thus inferring substantial energy savings, fast kinetics derive in the useof small

reactors and high methane conversions (≈90%) with elevatedselectivity towards hydrogen (94 ~ 99%). However, this process also presents some disadvantages such as high operating temperatures (900 ~ 1000°C), and the need for an oxygen plant, which makes this a highlycost process [11].

$$CH_{4(g)} + H_2O_{(g)} = 3H_{2(g)} + CO_{(g)} \quad (1)$$

$$2CH_{4(g)} + O_{2(g)} = 4H_{2(g)} + 2CO_{(g)} \quad (2)$$

In an attempt to solve these disadvantages research has been conducted in order to reduce production costs of syngas through POX and to lower operating temperatures. A proposed strategy is the elimination of the oxygen plant, which represents about half of the investment [12]. An example of such achievements is the use of metal oxides as oxygen carriers, based on a variation of the partial oxidation of methane to produce syngas and/or hydrogen involving two steps: first, the necessary oxygen for partial oxidation is provided by a metal oxide (MeO) containing oxygen, which is released under a reducing atmosphere to produce syngas and the reduced metal (Me) (Reaction 3); while in the second, the reduced metal is reoxidized with steam to produce hydrogen and the MeO (Reaction 4).

$$CH_{4(g)} + MeO = 2H_{2(g)} + CO_{(g)} + Me \quad (3)$$

$$H_2O_{(g)} + Me = MeO + H_{2(g)} \quad (4)$$

The MeO is then used again in reaction (3) to complete a full cycle, this process is called POX-MeO or chemical looping partial oxidation (CLPO) [5, 11]. It is important to notice that the overall reaction of this process is comparatively equal to the SMR [12]. TheCLPO system composed of two reactors.In the first reactor, called the fuel reactor, reaction (3) takes place, where a fuel such as methane is fed together with a fresh metal oxide (MeO). The gaseous products from the fuel reactor may include H_2, CO, CO_2 and H_2O, while the reduced oxygen carrier (Me) is the only solid product, which is sent to a second oxidation reactor where a gaseous oxidant (steam) reacts with the reduced metal through reaction (4) producing H_2 and the oxidized oxygen (OC) carrier (MeO), which is sent back to the fuel reactor to complete one full cycle of the OC. Partial oxidation of methane under this concept was first proposed by Ryden and Lyngfelt [13] and followed by Mattisson and Lyngfelt [14, 15]. Chemical looping partial oxidation (CLPO) allows for partial oxidation of the fuel using the metal oxide concept. In contrast, in a conventional partial oxidation only pure oxygen is used, while autothermal reforming uses both steam and oxygen.The reactions used in CLPO (reactions 3 and 4) are similar to conventional reforming and partial oxidation, except the metal oxide provides oxygen to the fuel. From reaction (4) only

a limited number of metals can be oxidized by steam, such as Fe, Co, Mn, Zn, Mo and W among others [16].

Processes that make use of this CLPO concept include the syngas chemical looping (SCL) process developed by Tong et al. [17] the iron-based IGCC process proposed by Cormos [18], the one-step decarbonization process envisioned by Mizia et al. [19] and the three-reactor scheme projected by Kang et al. [20]. Hydrogen production using steam to oxidize reduced iron employing solar energy to reduce this metal has also been reported by Nakamura [21]. Specifically, for the chemical looping process towards the production of syngas (CLPO), the main metal oxides studied have been Ce, Fe, and Ni.

Because of the many limitations (thermodynamics and kinetics) of single metal oxides, binary metal oxides have been proposed to enhance the selectivity of the oxygen carrier for syngas production. An example of these materials are mixed oxides with spinel structure, perovskite-type mixed oxides composed of transition metals that function not only as lattice oxygen carriers but also as catalysts for CH_4 activation as reported by Ryden et al. [22]. Mihai et al. [23] indicate that ceramic materials such as perovskite-type complex oxides (ABO_3)offer a well-defined structure and high thermal stability as oxygen carriers for CLPO applications and have been widely studied in some important areas of solid state chemistry, catalysis, advanced materials and physics. These researchers claim that the cation A is responsible for the high thermal resistance, while the high valence cations at the B site provide the catalytic activity. Therefore, both A and B cations can influence the stability of the perovskite structure as well as the reactivity and selectivity of lattice oxygen during the oxidation of CH_4. Examples of these perovskite materials include $LaFeO_3$, and $La_{0.7}Sr_{0.3}FeO_3$.

Furthermore, some researchers have centered their efforts in the synthesis of oxygen carrier materials for syngas production based in the so called concept of “solid diffusional reactive barrier” in order to avoid sintering effects in the material. This concept consists in a well-defined crystalline structure of a mixed-metal oxide that when exposed to a reducing environment such as CH_4, this changes to reduced metallic species. Then, when these reduced metallic mixture is reoxidized using, steam, these come back to its original crystalline structure. The reconstitution of the original crystalline structure is thought to be responsible for the high thermal stability of these materials avoiding sintering effects, responsible for the reduction of activity when oxygen carriers are exposed to several reduction-oxidation cycles. Examples of these type of materials include iron-titanium metal oxide (Fe_2TiO_5) proposed by Luo et al. [24] for the oxidation of methane under a CLPO scheme. Thermodynamic simulations and experimental results have confirmed that the CLPO chemical looping process using the Fe_2TiO_5 oxygen carrier is capable of producing >90% purity syngas at nearly a 2:1H_2:CO ratio. Furthermore, De los Rios et. al [2, 11, 25] proposed cobalt tungstate ($CoWO_4$) together with a nickel catalyst as an oxygen carrier for

CLPO to produce high purity syngas and found that this material is very stable to cyclic tests subjected to partial oxidation of methane to syngas production.

Between these two materials $CoWO_4$ is a very remarkable material, since the reduced form of Fe_2TiO_5 with methane is reported to lead to a mixture of Fe and $FeTiO_3/Fe_2TiO_4$ [24]. Whereas, the reduction of $CoWO_4$ produces only Co and W metallic species and these when reoxidized with steam generate $CoWO_4$ again.

Following this innovative concept, a number of other possible tungstate species are feasible to be considered under these moieties. For example, tungstate species having the structure $MWO_4$are expected to produce syngas during the reduction step with CH_4 and be reoxidized back again with steam according to the following reactions:

$$4CH_{4(g)} + MWO_4 \rightarrow 8H_{2(g)} + 4CO_{(g)} + M + W \quad (5)$$

$$CH_{4(g)} + MWO_4 \rightarrow 2H_2O_{(g)} + CO_{2(g)} + M + W \quad (6)$$

$$CH_{4(g)} \rightarrow C + 2H_{2(g)} \quad (7a)$$

$$2CO_{(g)} \rightarrow C + CO_{2(g)} \quad (7b)$$

$$4H_2O_{(g)} + M + W \rightarrow MWO_4 + 4H_{2(g)} \quad (8)$$

$$C + H_2O_{(g)} \rightarrow H_{2(g)} + CO_{(g)} \quad (9a)$$

$$C + 2H_2O_{(g)} \rightarrow 2H_{2(g)} + CO_{2(g)} \quad (9b)$$

Where M = Fe, Mn or Ni. The POX-MeO-1 reaction (5) produces syngas (CO + H_2) together with M and W reduced metallic species, while POX-MeO-2 reaction (6) describes the possible complete oxidation of methane to produce CO_2 and H_2O. Under these oxygen starving conditions, other reactions may arise such as coal formation reactions 7(a) and 7(b), which correspond to the methane decomposition and Boudard reactions, respectively. The reoxidation of the metallic Co and W species with steam is described by reaction (8) to produce the MWO_4 oxygen carrier and H_2, while if some carbon may have formed according to previous reactions 7(a) and 7(b), coal gasification reactions (9a) and (9b) may occur during the reoxidation stage leading to further hydrogen production and carbon oxide species (CO and CO_2).

Due to the remarkable reaction behavior of the $CoWO_4$ oxygen carrier towards the production of syngas from methane and the reoxidation of its reduced species (Co and W)

with steam to further produce H_2, makes this reaction concept very attractive to be evaluated using other metallic tungstates such as $FeWO_4$, $MnWO_4$ and $NiWO_4$under a CLPO reaction scheme. Therefore, the aim of the present study is to evaluate the feasibility of these tungstate metal oxides through the use of thermodynamic analyses performed by process simulations to evaluate the feasibility of these tungstate oxides to be used under a chemical looping partial oxidation (CLPO) reaction scheme for the production of hydrogen and/or syngas.

2. Methodology

Process Simulation

Concentration at equilibrium calculations in the CLPO for the MWO_4 oxygen carriers will be performed using the RGIBBS reactor model from Aspen Plus© process simulation software. This reactor model has been successfully employed in the simulation of several chemical looping reaction systems [26, 27, 28 and 29]. Thisreactor model is able to determine the equilibrium amount of all different possible product species as well as their phases (gas, solid and liquid). For the methane partial oxidation (fuel reactor) and H_2 production (steam oxidation reactor) systems the gaseous species included were: CH_4, CO, CO_2, H_2, and H_2O, while solid species included: C, $NiWO_4$, $MnWO_4$, $FeWO_4$, Ni, Fe, Mn, W, WO_2 and WO_3. The RGIBBS module is based on the Gibbs free energy minimization technique (also called the nonstoichiometric method), details of this method can be found elsewhere [30, 31].

Process simulations using Aspen Plus© will concentrate in determining process material and energy balances, as well as optimal operating conditions in both reactors and in the entire process [1, 31].During the thermodynamic simulation work, process simulation variables studied were: fuel reactor temperature, which varied from 100-1000 °C at 1 atm, MWO_4 molar feed, which varied from 1 to 3 kmol/h, while fixing 4 kmol/h of CH_4. Whereas, in the oxidation reactor H_2O molar feed rate was varied from 3 to 9 kmol/h, in a temperature range of 200-700 °C. Other simulation conditions employed include: the use of a thermodynamic system based on the Redlich-Kwong-Aspen equation of state (EOS) to calculate the physical properties of the chemical species employed, which is an adequate EOS in processes involving hydrocarbons and their mixtures with polar components, and combinations of small and large molecules or hydrogen-rich systems at medium and high pressures [32]. Also, the calculation basis for CH_4 feed to the fuel reactor was fixed at 4 kmol/h, while calculations in the fuel reactor aimed for conditions where no carbon formation was allowed. It is important to state that all the present simulation calculations are based on theoretical thermodynamic considerations and these are to be taken as a guide to further experimental evaluation of the reaction CLPO process, since no

heat and mass diffusional limitations as well as kinetics effects were taken into account for the conformation of the present thermodynamic and process analysis.

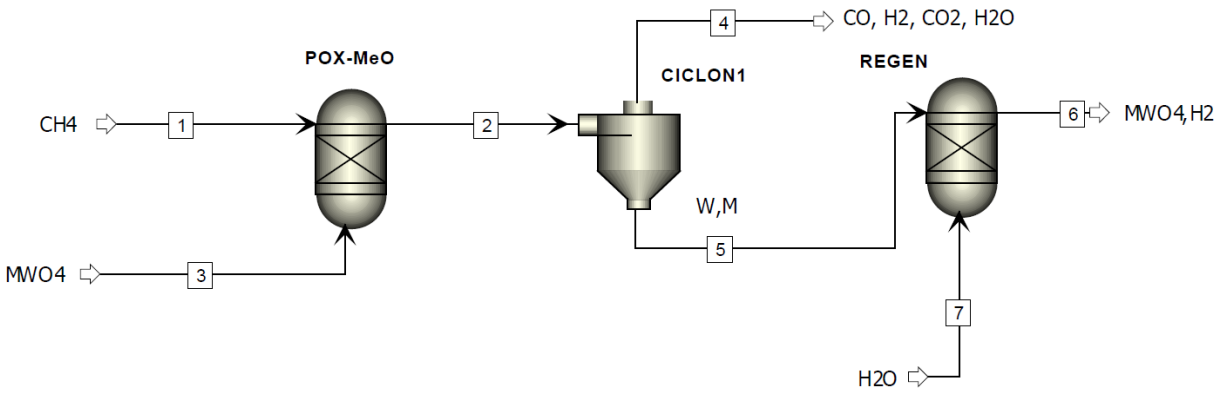

Figure 1. Process simulation flowsheet

The CLPO process for MWO_4(M = Fe, Ni) OC scheme is shown in Figure 1. Here, the reactors used (POX-MeO and REGEN) used the RGIBBS model. In the first fuel (POX-MeO), the oxidation of methane in the presence of the tungstate oxide (MWO_4) takes place, while in the second (REGEN reactor) tungsten and the reduced metal reoxidation reactions occur in the presence of steam, thus regenerating the tungstate oxide and producing hydrogen, as well as the removal of any carbon deposits on the oxygen carrier. A cyclone at the outlet of the first reactor (CICLON1)is used to separate the solid and gaseous products resulting from this reactor. In the case of the first separation, the expected resulting solids from the POX-MEO reactor (M, tungsten, and a possible small fraction of deposited carbon) are carried out as reagents for the second reactor (REGEN) and the separated gas (stream 4) constitutes the syngas. In the REGEN reactor, according to reactions (8), (9a) and (9b), the solid products andthe tungstate oxide (stream 6) constitute a hydrogen-rich product.

In order to find optimal variables of the CLPO process, several sensitivity analyzes will be performed and these are aimed to obtain the highest yield towards syngas (CO + H_2) in the fuel reactor, while avoiding carbon formation and to produce a rich hydrogen gaseous stream in the oxidation reactor. The first sensitivity analysis is performed in the fuel reactor aiming to find the molar feed of MWO_4 to react with 4 kmol/hr of CH_4 to produce the maximum amount of syngas (CO + H_2), while avoiding carbon formation. Also, in the same sensitivity analysis the temperature of this operation is varied to determine the optimal temperature to obtain the highest yield towards syngas production. The second sensitivity analysis is to be carried out in the steam oxidation reactor by studying the variation of the operating temperature and the molar flow of steam feed to achieve complete regeneration

of MWO_4 from the solid reaction products comingfrom the fuel reactor (M and W species) with steam to produce a rich hydrogen gaseous stream. Once the optimal operating variables of the simulation are determined, the resulting mass and energy balances of the process are established.

3. Results and Discussion

Thermodynamic Analysis

Figure 2 presents results from a thermodynamic analysis consistingin the calculation of the equilibrium amounts within the POX-MEO reactor using the RGIBBS model using a CH_4molar feed of 4 kmol/h.

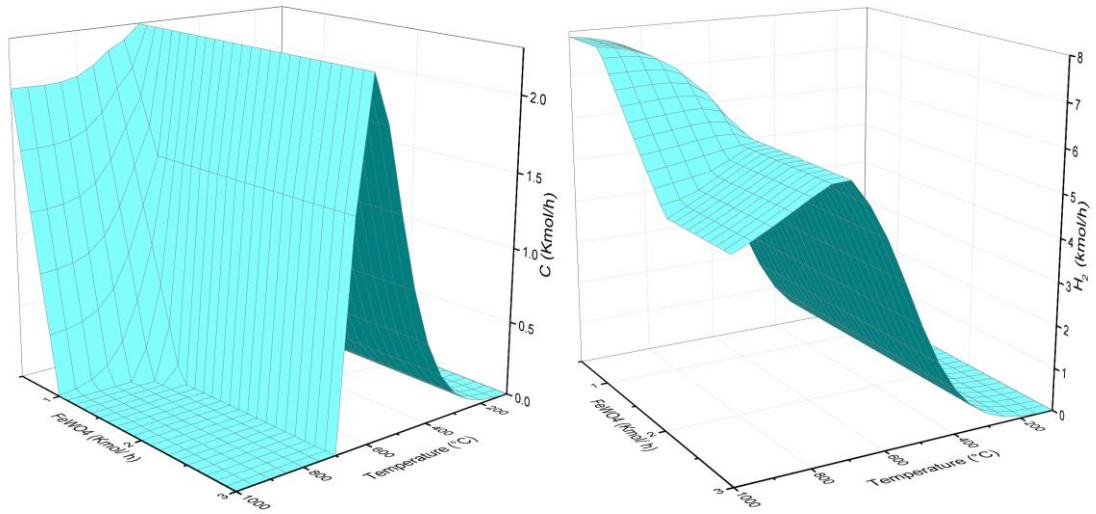

Figure 2. Thermodynamic analysis of the POX-MEO reactor with $FeWO_4$, C (left) and H_2 (right)).

In Figure 2 the carbon formation C (kmol/h) is plotted as a function of the $FeWO_4$ feed (kmol/h) and temperature (°C). In this Figure it is evident that the null generation of deposited carbon in the reaction products from the POX-MEO reactoris comprised in a region from 700 °C and 1.4-3 kmol/h of $FeWO_4$ and 1000 °C and 1.2 kmol/h of $FeWO_4$. Within this region according to Figure 2 the maximum hydrogen production that can be achieved is 6.51 kmol/h of H_2 at 750 °C and 1.5 kmol/h of $FeWO_4$.

Otherwise, Figure 3 shows results from the thermodynamic analysis of the $MnWO_4$ oxygen carrier in the POX-MeO reactor. Again, in this Figure the generation of deposited carbon

and the hydrogen production is plotted as a function of $MnWO_4$ feed in kmol/h and temperature (°C).

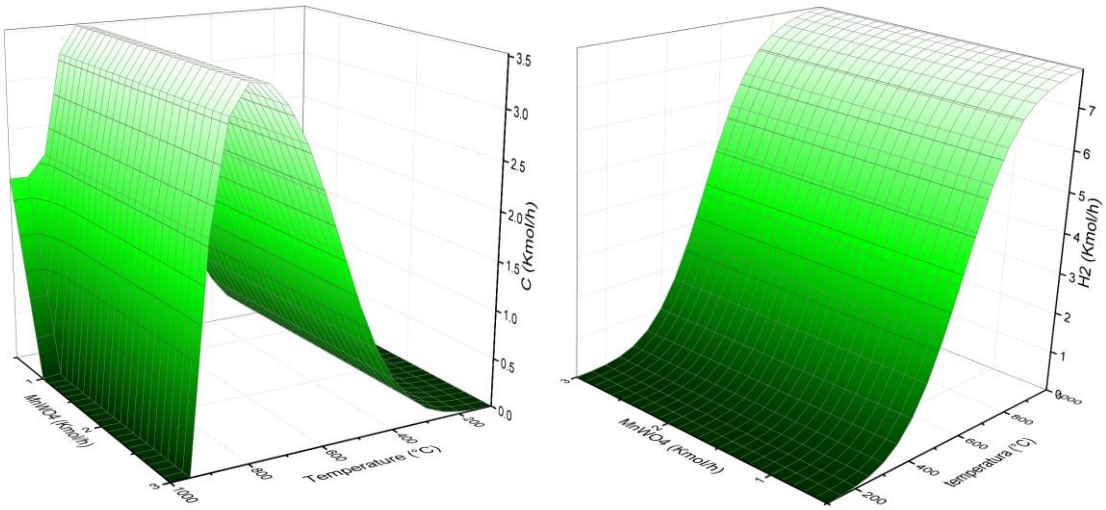

Figure 3. Thermodynamic analysis of the POX-MEO reactor with $MnWO_4$, C (left) and H_2 (right)).

In this Figure it is apparent that no carbon formation within the reaction products from the POX-MEO reactor is generated in a square small region formed at 950-1000 °C and 1.1-3 kmol/h of $MnWO_4$. While, maximum hydrogen production within this small region is of 7.83 kmol/h of H_2 at 950 °C and 1.1 kmol/h of $MnWO_4$.

Moreover, Figure 4 shows results from the thermodynamic analysis of the $NiWO_4$ oxygen carrier in the POX-MeO reactor. In this Figure the formation of deposited carbon and the hydrogen production is plotted as a function of $NiWO_4$ feed in kmol/h and temperature

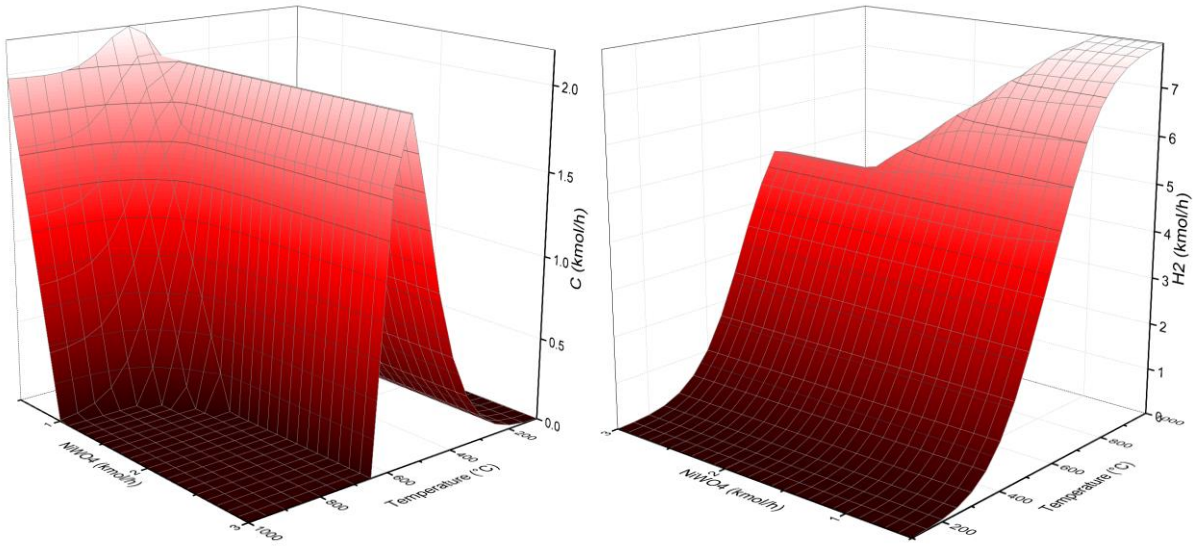

(°C).

Figure 4. Thermodynamic analysis of the POX-MEO reactor with $NiWO_4$, C (left) and H_2 (right)).

In Figure 4 the carbon formation C (kmol/h) is plotted as a function of the $NiWO_4$ feed (kmol/h) and temperature (°C). In this Figure it is evident that no generation of deposited carbon in the reaction products from the POX-MEO reactor is included in a region from 700°C @ 3 kmol/h of $FeWO_4$ and 650 °C@ 3 kmol/h of $NiWO_4$. Within this region according to Figure 4 the maximum hydrogen production that can be achieved between 700°C @ 1.5 kmol/h $NiWO_4$and650°C@ 3kmol/h $NiWO_4$, where the H2 production varies from 5.98 to 6.62 kmol/h of H_2, respectively.

According to results from Figures 2-4 maximum free-carbon hydrogen production can be achieved by either $FeWO_4$or $NiWO_4$ oxygen carriers. It is important to note that even though both oxygen carriers produce an important amount of H_2 within the no carbon formation region, $NiWO_4$ presents a wider range of operation for the production of hydrogen. Furthermore, reduced Ni according to POX reaction (5) will produce metallic Ni, which is a very well-known active metal catalyst for the dry as well as for the steam reforming of methane.

Therefore, due to these previous results and convenient features, it was concluded that $NiWO_4$ is the best oxygen carrier among the studied tungstate materials for the production of H_2 and/or syngas based on theoretical thermodynamics point of view.

Figure 5 and 6 present other the production of CO, CO_2andW and Ni, respectively based on $NiWO_4$ as oxygen carrier for the POX-MeO reactor.

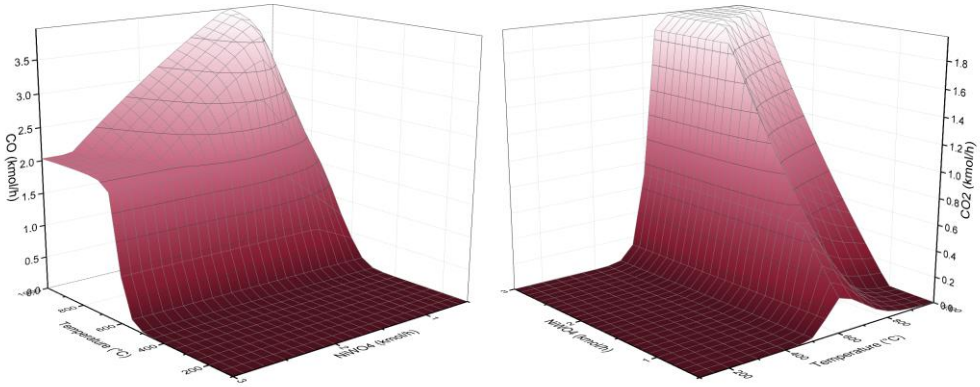

Figure 5. Thermodynamic analysis of the POX-MEO reactor with $NiWO_4$, CO (left) and CO_2 (right)).

Results of Figure 4and 5 show that a maximum of 6.8 kmol/h of hydrogen can be obtained and combined with 2.6 kmol/h of CO at a temperature of 700 ° C and a production of 1.7 kmol/h of W and also of Ni, thus avoiding carbon generation. These results can also be observed in Figure 6 where the production of Ni and Win the reduction reactor is shown.

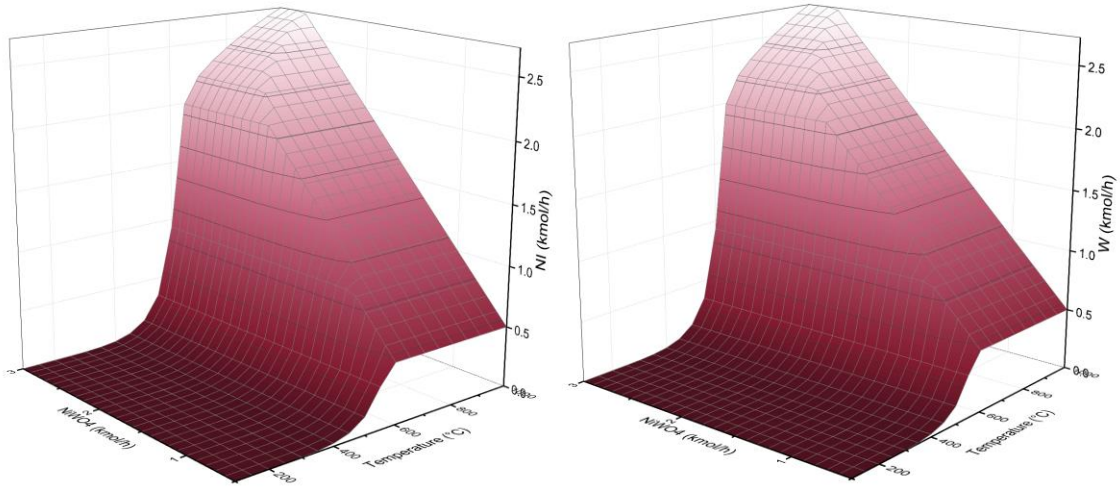

Figure 6. Thermodynamic analysis of the POX-MEO reactor with $NiWO_4$, Ni (left) and W (right)).

Results of this analysis reveal that high temperatures promote syngas production (H_2 + CO) in the product gas, while keeping the H_2/CO molar ratio equal or greater than 2 as shown in Figures 4 and 5. This is expected since at high temperatures the partial oxidation of methane by $NiWO_4$ is an endothermic reaction, which implies that this reaction (5) governs the thermodynamic system of gaseous species within the fuel reactor. On the other hand, solid products from this fuel reactor as a function of temperature as shown in Figure 6. Here, it is possible to observe that in order to avoid carbon formation, it is necessary to raise the temperature to more than 650 ° C. Also, in Figure 6 it can be seen that greater temperatures than 400 °C will lead to formation of Ni and W, while greater temperatures than 675 °C will

produce greater amounts of these reduced metallic species (Ni and W).

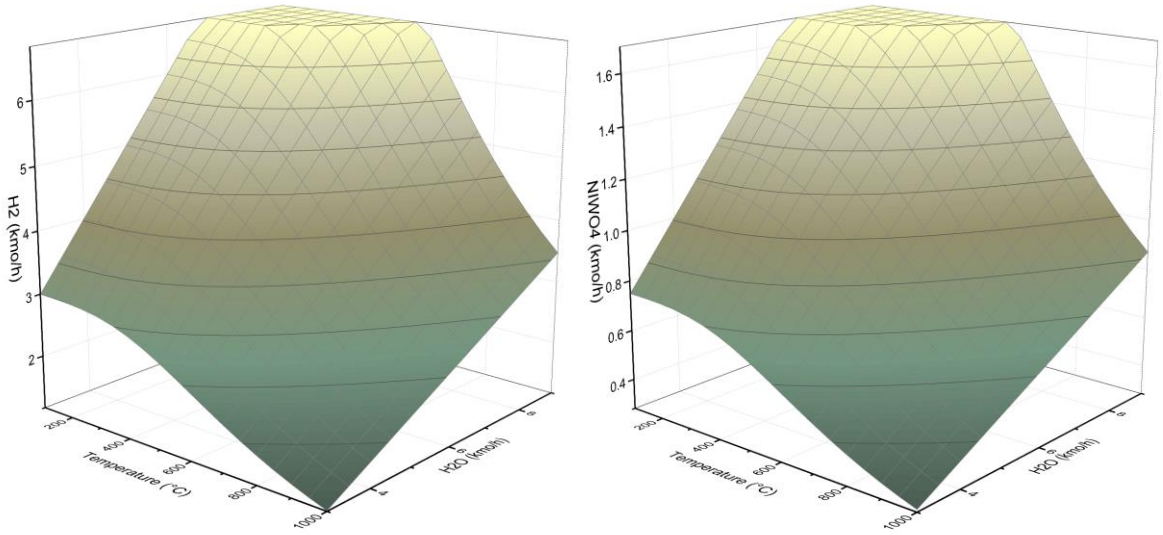

Figure 7. Thermodynamic analysis of the REGEN reactor with $NiWO_4$, H_2 (left) and $NiWO_4$ (right)

Figures 7 presentsresults from a thermodynamic analysis consisting in the calculation of the equilibrium amounts within the REGEN reactor using the RGIBBS model using H_2O (steam) as molar feed. In this Figure the production of H_2 and $NiWO_4$is plotted as a function of a range oftemperature of 100-1000 °C and a steam feed of 2-9 kmol/h.In this reactor the solid products from thereduction reactor consisting of 1.7 kmol/h of both W and Ni were also fed.

From this Figure it can be seen that oxidation of the reduced metals (Ni and W) to form$NiWO_4$ is feasible at relatively low temperatures (even below 300 °C) and at a maximum H_2 generation of 6.8kmol/h at 7 kmol/h of H_2O feed. However, in order to favor the reaction kinetics of reaction (8), it is convenient to use temperatures above 500 °C. This condition allows a reasonable small temperature gradient between the two reactors.

According to the results shown in figure 7 it was observed that the most suitable operating temperature for the regeneration reactor is in the range of 100-550 °C and more specifically at 500 °C since inthis range the nickel tungstate generation is stable with a production of 1.7 kmol/h,while a maximum production of H_2 of 6.8 kmol/h is obtained at a feed of 8.5 kmol/h of water vapor. Thus, the optimum operating conditions selected for the second reactor is 500 °C, which according to Figure 7 corresponds to a molar steam feed flow of 6.5 kmol/hr and producing 1.7 kmol/h of $NiWO_4$ and 6.8 kmol/h of H_2.

Therefore, it can be concluded thatin the reduction reactor (POX-MeO) for the synthesis gas production optimal operating conditions of this reactor are as follows: a temperature of 700°C and a feed of 4 kmol/h of CH_4 and 1.7 kmol/h of $NiWO_4$.The established operating temperature of 700 °C in the first reactor, where the partial oxidation of methane occurs, is relatively lower than those reported with other oxygen carrier materials and this represents potential energy savings. Meanwhile in the regeneration reactor (REGEN)optimum operating conditions are 500 °C anda feed of 1.7 kmol/h of Ni, 1.7 kmol/h of W and 8.5 kmol/h of steam to produce 1.7 kmol/h of $NiWO_4$and 6.8 kmol/h of H_2.

Within the simulation, once the appropriate parameters for the entire process were established through the sensitivity analyzes, it was possible to obtain the results shown in Table 1.

Table 1. Simulation results according to Figure 1.

Stream	1	2	3	4	5	6	7
Temperature, °C	25	750	0	750	0	500	25
Pressure, bars	2.026	2.026	2.026	1.013	1.013	2.026	2.026
Vapor Fraction	1	364.81	459.806	1	363.81	451.516	0
Molar Flow, kmol/hr	4	11.803	0	11.803	0	6.5	6.5
Mass Flow, kg/hr	64.171	160.167	0	160.167	0	30.393	117.099
Volume Flow, m^3/hr	97.692	991.167	0.045	991.143	0.024	412.518	0.118
Enthalpy Gcal/hr	-0.071	-0.168	0	-0.168	0	-0.04	-0.449
molar Flow kmol/hr	0	3	1.5	0	3	1.645	0
H_2	0	6.513	0	6.513	0	5.419	0
CO	0	3.092	0	3.092	0	0	0
CO_2	0	0.809	0	0.809	0	0	0

H_2O	0	1.289	0	1.289	0	1.081	6.5
W	0	1.5	0	0	1.5	0.145	0
C	0	0	0	0	0	0	0
CH_4	4	0.099	0	0.099	0	0	0
$NIWO_4$	0	0	1.5	0	0	1.355	0
NI	0	1.5	0	0	1.5	0.145	0
Mass Flow, kg/hr	64.171	523.977	459.806	160.167	363.81	480.909	117.099
Enthalpy, Gcal/hr	-0.071	0.0019	-0.808	-0.168	0.034	-0.728	-0.449

These results show the production of synthesis gas in the first reactor of reduction of $NiWO_4$, whereas in the regeneration reactor a production of hydrogen results from the oxidation of the previously reduced metals.

4. Conclusions

Different types of MWO_4 (M = Fe, Mn, Ni) were evaluated through thermodynamic analysis and process simulation for the production of hydrogen-synthesis gas (syngas) using Aspen Plus. According to the thermodynamic analysis results, it is concluded that $NiWO_4$ is the best oxygen carrier among the studied tungstate materials for the production of H_2 and/or syngas. Simulation results found at the exit of the reduction reactor a free carbon deposition window located between a feed range of 1.6-3 kmol/h of $NiWO_4$ and a temperature range of 100-1000 °C. While the working window in which no coal is produced is at a temperature range of 700-1000 °C at a feed range of 1.7-3 kmol/h of $NiWO_4$. Within the reduction reactor the H_2/CO molar ratio of the synthesis gas is from 2.5-2.7 kmol/h and producing from 1.6-2 kmol/h of W, with a maximum of 1.7 kmol/h at a temperature of 700 °C. While in regeneration reactor there is a reduced range of temperatures, consisting of 100-550 °C at a feed of 6-9 kmol/h of steam and more specifically at 500 °C with a feed of steam of 8.5 kmol/h. Finally, it is concluded that relatively moderate temperatures such as 700 °C and a $NiWO_4$ feed of 1.6-3 kmol/h are needed to generate carbon-free synthesis gas. While in the regenerator 1.7 kmol/h of $NiWO_4$ is obtained at a temperature of 500 °C, while producing 6.8 kmol/h of H_2.

References

[1] BP Energy Outlook 2035, available at: http://www.bp.com/es_es/spain/conozca-bp/informes-y-publicaciones/bp-energy-outlook.html

[2] Sunny A., Solomon P.A., Aparna K., Syngas production from regasified liquefied natural gasand its simulation using Aspen HYSYS. J. Nat. Gas Sci. Eng. 2016. 30: p. 176-181.

[3] De Los Ríos T., Delgado Vigil M.D., Collins-Martinez V., Lopez Ortiz A., Synthesis,characterization and stability performance of CoWO4 as an oxygen carrier under redox cyclestowards syngas production. Int. J. Chem. Reactor Eng. 2007. 5(1): p. 1-12.

[4] Wilhelm DJ., Simbeck D.R., Karp AD., Dickenson RL., Syngas production for gas-to-liquidsapplications: technologies, issues and outlook. Fuel Process. Technol. 2001. 71(1–3): p. 139-148.

[5] Vázquez Sosa MI., Delgado Vigil MD., Salinas Gutiérrez J., Collins-Martínez V., LópezOrtiz A., Synthesis gas productionthroughredoxcycles of bimetallic oxides and methane. J.New Mater. Electrochem. Syst. 2009. 12: p. 029-034.

[6] Haarlemmer G., Bensabath T., Comprehensive Fischer–Tropsch reactor model with non-idealplug flow and detailed reaction kinetics. Comput. Chem. Eng. 2016. 84: p. 281-289.

[7] Dincer I., Acar C., Review and evaluation of hydrogen production methods for bettersustainability. Int. J. Hydrogen Energy. 2015. 40(34): p. 11094-11111.

[8] Jansen D., Gazzani M., Manzolini G., Carbo MC., Pre-combustion CO2 capture. Int. J. Greenhouse Gas Control. 2015. 40: p. 167-187.

[9] Makarshin LL., Sadykov VA., Andreev DV., Gribovskii AG., Privezentsev VV., Parmon VN. Syngas production by partial oxidation of methane in a microchannel reactor over a Ni–Pt/La0.2Zr0.4Ce0.4Ox catalyst. Fuel Process. Technol. 2015. 131: p. 21-28.

[10] Voldsund M., Jordal K., Anantharaman R. Hydrogen production with CO_2 capture. Int. J. Hydrogen Energy. 2016. 41(9): p. 4969-4992.

[11] De los Ríos Castillo T., Salinas Gutiérrez J., López Ortiz A., Collins-Martínez V. Global kinetic evaluation during the reduction of $CoWO_4$ with methane for the production of hydrogen. Int. J. Hydrogen Energy. 2013. 38(28): p. 12519-12526.

[12] Protasova L., Snijkers F. Recent developments in oxygen carrier materials for hydrogen production via chemical looping processes. Fuel, 2016. 181: p. 75-93.

[13] Rydén M., Lyngfelt A. Using steam reforming to produce hydrogen with carbon dioxide capture by chemical-looping combustion. Int. J. Hydrogen Energy. 2006, 31: p.1271–1283.

[14] LyngfeltA,.Mattisson T. Trestegsf¨orbr¨anningf¨oravskiljningavkoldioxid. Patent-ochregistreringsverket, Sweden, 2005.

[15] Mattisson T., Lyngfelt A., Leion H. Chemical-looping with oxygen uncoupling for combustion of solid fuels. Int. J. Greenhouse Gas Control. 2009, 3: p. 11–19.

[16] Svoboda K., Siewiorek A., Baxter D., Rogut J., Pohorely M. Thermodynamic possibilities and constraints for pure hydrogen production by a nickel and cobalt-based chemical looping process at lower temperatures. Energy Convers Mgmt 2008, 49: p. 221–231.

[17] Tong A., Sridhar D., Sun Z., Kim HR., Zeng L., Wang F., Wang D., Kathe MV., Luo S., Sun Y. Continuous high purity hydrogen generation from a syngas chemical looping 25kWth sub-pilot unit with 100% carbon capture. Fuel 2013, 103: p. 495–505.

[18] Cormos CC. Hydrogen production from fossil fuels with carbon capture and storage based on chemical looping systems. Int. J. Hydrogen Energy 2011, 36: p. 5960–5971.

[19] Mizia F., Rossini S., Cozzolino M., Cornaro U., Tlatlik S., Kaus I., Bakken E., Larring Y. One step decarbonization. In: Eide LI, ed. Carbon Dioxide Capture for Storage in Deep Geologic Formations, vol. 3. Berkshire: CPL Press; 2009.

[20] Kang K-S., Kim C-H., Bae K-K., Cho W-C., Jeong S-U., Lee Y-J., Park C-S. Reduction and oxidation properties of Fe_2O_3/ZrO_2 oxygen carrier for hydrogen production. Chem. Eng. Res. Des. 2014, 92(11): p. 2584–2597.

[21] Nakamura MT. Hydrogen production from water utilizing solar heat at high temperatures. Solar Energy 1977, 19: p. 467–475.

[22] Rydén M., Leion H., Mattisson T., Lyngfelt A. Combined oxides as oxygen-carrier material for chemical-looping with oxygen uncoupling. Appl. Energy 2014;113: p. 1924–32.

[23] Mihai O.., Chen D., Holmen A. Catalytic consequence of oxygen of lanthanum ferrite perovskite in chemical looping reforming of methane. Ind. Eng. Chem. Res. 2011;50: p. 2613–21.

[24] Luo S., Zeng L., Xu D., Kathe M., Chung E., Deshpande N., Qin L., Majumder A., Hsieh T-L, Tong A. Shale gas-to-syngas chemical looping process for stable shale gas conversion to high purity syngas with a H_2:CO ratio of 2:1. Energy Environ. Sci. 2014, 7: p. 4104–4117.

[25] De Los Ríos-Castillo, T., Cortez Palacios L., De los Ríos SA., Delgado Vigil D., Salinas Gutiérrez J., López Ortiz A., Collins-Martínez V. Study of $CoWO_4$ as anOxygenCarrierfortheProduction of HydrogenfromMethane. J. New Mater. Electrochem. Sys. 2009. 12(1): p. 55-61.

[26] Mehrpooya, M., Sharifzadeh MMM., Rajabi M., Aghbashlo M., Tabatabai M., Hosseinpour S., Ramakrishna S. Design of an integrated process for simultaneous

chemical looping hydrogen production and electricity generation with CO_2 capture. Int. J. Hydrogen Energy, 2017. 42(12): p. 8486-8496.

[27] Antzara, A., Heracleous E., Bukur DB., Lemonidou AA. Thermodynamic analysis of hydrogen production via chemical looping steam methane reforming coupled with in situ CO_2 capture. Int. J. Greenhouse Gas Control, 2015. 32: p. 115-128.

[28] Meng, W.X., Banerjee S., Zhang X., Agarwal RK. Process simulation of multi-stage chemical-looping combustion using Aspen Plus. Energy, 2015. 90: p. 1869-1877.

[29] Zhou L., Zhang Z., Agarwal RK. Simulation and validation of chemical-looping combustion using ASPEN plus. Int. J. Energy Environ, 2014. 5(1): p. 53-59.

[30] Collins-Martínez V., Escobedo Bretado M., Meléndez Zaragoza M., Salinas Gutiéerrez J., López Ortiz A. Absorption enhanced reforming of light alcohols (methanol and ethanol) for the production of hydrogen: thermodynamic modeling. Int. J. Hydrogen Energy 2013. 28: p. 12539-53.

[31] Sandler SI., Using Aspen Plus in thermodynamics instruction: a step-by-step guide. 2015: John Wiley & Sons.

[32] Mathias PM. A versatile phase equilibrium equation of state. Ind. Eng. Chem. Process Des. Dev., 1983. 22(3): p. 385-391.